Density Functional Theory and Molecular Clusters

PAVEL HOBZA,* JIŘÍ ŠPONER, and TOMÁŠ RESCHEL†

J. Heyrovský Institute of Physical Chemistry, Academy of Sciences of the Czech Republic, Dolejškova 3, 182 23 Prague 8, Czech Republic. E-mail: HOBZA@INDY.JH-INST.CAS.CZ

Received 9 November 1994; accepted 13 March 1995

ABSTRACT

Density functional theory (DFT) methods, including nonlocal density gradient terms in the exchange and correlation energy functionals, were applied to various types of molecular clusters: H-bonded, ionic, electrostatic, and London. Reliable results on the structure and stabilization energy were obtained for the first two types of cluster as long as Becke3LYP and Becke3P86 functionals and basis sets of at least DZ + P quality were used. DFT methods with currently available functionals failed completely, however, for London-type clusters, for which no minimum was found on the potential energy surfaces. DFT interaction energy exhibits the same basis set extension dependence as the Hartree-Fock (HF) interaction energy. Therefore, the Boys-Bernardi function counterpoise procedure should be employed for elimination of the DFT basis set superposition error.

Introduction

Accurate calculations on various types of molecular clusters are tedious. The conventional Hartree-Fock (HF) method is applicable only for ionic and H-bonded clusters, and even for these clusters the correlation energy plays a non-negligible role. Passing to London clusters (dominated by the dispersion energy), the correlation energy becomes by far the most important attractive contribution. It is not easy to describe accurately the attraction in these clusters within the HF plus electron correlation methods due to the slow convergency of the correlation energy with the basis set. Alternate computational methods based, for example, on the density functional theory (DFT) therefore attract a growing interest among theoreticians working with molecular clusters.

The DFT method emerged from solid-state physics, and solid-state electronic calculations contributed to the initial success of the method. Two features make DFT methods attractive: (1) They include at least some part of the electron correlation; and (2) they are not as computationally demanding as traditional molecular orbital (MO) methods because their cost increases only with the

*Author to whom all correspondence should be addressed.
†Undergraduate student at the Department of Physical Chemistry, Charles University, Prague.

CCC 0192-8651 / 95 / 111315-11

third power of the number of basis functions. Encouraging results for isolated molecules were obtained with DFT methods only when these methods went beyond the local density approximation by incorporating nonlocal, density-gradient terms in the exchange and correlation energy functional.[2,3] The first applications of DFT methods in the field of molecular clusters included H-bonded clusters [the water dimer and formamide ··· water,[4] small water clusters,[5] ammonia dimer,[6] $(H_5O_2)^+$ cluster,[7] formamide dimer,[8a] $NH_3 \cdots NH_4^+$, $(H_2O)_2$ and $(CH_3OH)_2$,[8b] $(H_2O)_2$,[8c] adenine ··· thymine and guanine ··· cytosine pairs,[8d] and $(Au^+ \cdots OH_2)$ ionic clusters[9]]. The structure of H-bonded clusters agreed with HF or HF+ correlation energy treatments and with experimental results. It was concluded that nonlocal DFT resutls are closer to those obtained using *ab initio* treatments that include electron correlation. DFT stabilization energy was shown[4] to possess a small value of the basis set superposition error (BSSE); a clear conclusion about the use of the function counterpoise method of Boys and Bernardi[10] is, however, still lacking.

Considerably less is known about the applicability of DFT for other types of molecular clusters. It is suspected that the dispersion energy is not properly considered in the DFT method, and therefore any success of the method with dispersion-energy-dominated clusters (London clusters) is fortunate.

The aim of this article is to study the applicability of DFT methods for H-bonded, ionic, electrostatic, and London clusters, focusing on the proper use of the function counterpoise method for evaluating the interaction energy.

Computation

For the DFT calculations, we used the GAUSSIAN 92 code, which included the DFT methods.[12] Three various functionals containing gradient corrections for both exchange and correlations were used: BLYP,[13-15] Becke3LYP,[16] and Becke3P86.[17] Unless otherwise stated, the standard 6–31G*, 6–31G**, 6–31 + + G**, 6–311G*, D95**, and D95(2*d*, 2*p*) basis sets [12] were used. The structure of a cluster was determined either by gradient optimization (analytic gradient) or by the point-by-point method. The stabilization energy was evaluated with and without inclusion of the function counterpoise method.[10] The full function counterpoise method was considered (i.e., all the occupied and virtual orbitals of the ghost atom were considered). In case of gradient optimization, the BSSE was evaluated for the optimized structure; the reorganization energy was taken into account. Harmonic vibrational frequencies were calculated analytically.

The following clusters were studied:

1. H-bonded clusters: $(H_2O)_2$, $(HF)_2$, $(HCl)_2$, formamide ··· formamidine
2. Ionic clusters: $Li^+ \cdots OH_2$, $F^- \cdots OH_2$
3. Electrostatic clusters: $(benzene)_2$, $(ethylene)_2$
4. London clusters: $(Ne)_2$, $(Ar)_2$, benzene ··· Ar, benzene ··· Ne.

The structures of the clusters studied are presented in Figure 1.

Results and Discussion

HYDROGEN-BONDED CLUSTERS

Water Dimer

The geometry and energy characteristics of the linear C_s structure of the water dimer (Fig. 1a) evaluated with various functionals and various basis sets are summarized in Table I. Only in the Becke3P86 functional do all the optimized structures correspond to the energy minima. For the BLYP and Becke3LYP functionals, the 6–31G* and 6–31G** optimized structures posses one imaginary frequency (i.e., they correspond to the saddle points; this result does not agree with the *ab initio* data; see later in this article). We tried to localize the respective global minima but did not succeed. Passing to larger basis sets, the respective optimized structures have all the frequencies positive (i.e., they correspond to energy minima). It is clear from Table I that the geometry characteristics vary only slightly when passing from the BLYP functional to other functionals. In addition, the basis set dependence is not pronounced. The prolongation of the OH bond upon formation of the H bond is almost constant and does not depend on the functional or basis set. Similar geometry characteristics were also found in ref. 4 when nonlocal DFT functionals were applied. Introduction of BSSE reduces the stabilization energy and, as with the *ab initio* method, the BSSE is larger for smaller basis sets.

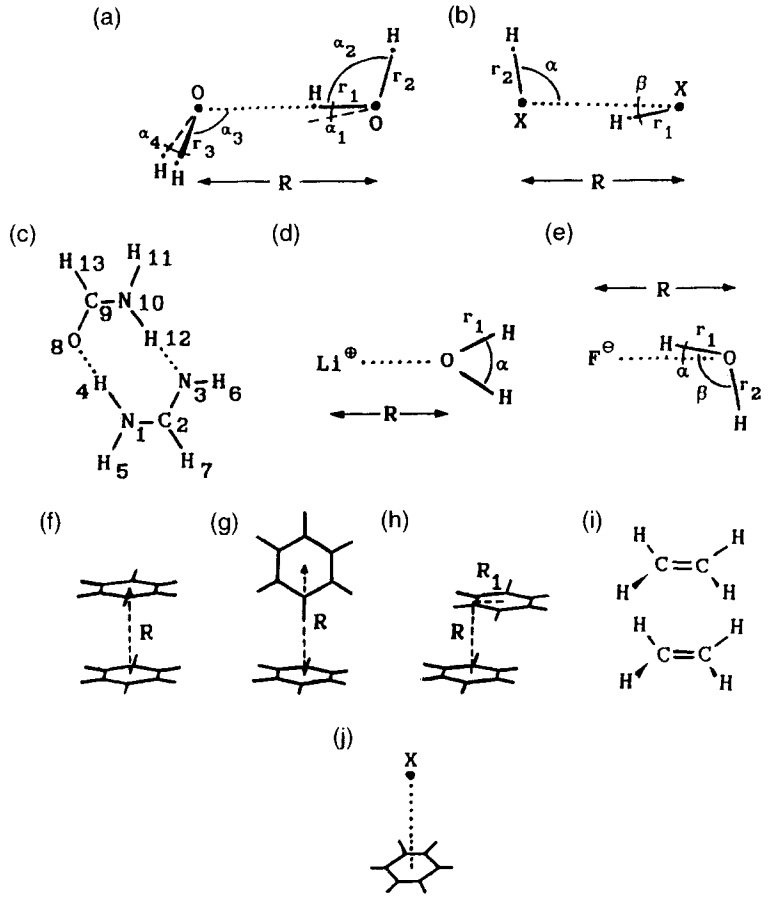

FIGURE 1. Structures of molecular clusters studied.

The water dimer has frequently been studied using various MO methods; the global minimum corresponds to the linear structure of the dimer. The *ab initio* stabilization energy converges[18-20a] to about 5.0 kcal/mol. The MP4 stabilization energy and BSSE-corrected MP4 stabilization energy evaluated with the extended basis set are 5.3 and 4.6 kcal/mol, respectively. The MP2 geometry calculated with the extended basis set[18] is as follows: R(2.92 Å), Δr (0.002 Å), α_1 (4°), α_3 (129°).

The DFT stabilization energies evaluated with the largest basis sets agree well with the MP4 stabilization energies. The DFT intermolecular distances are underestimated (by 0.06 Å), while the OH bond prolongation upon formation of the H bond is overestimated (see also ref. 11).

$(HF)_2$ and $(HCl)_2$

Gradient optimization of $(HF)_2$ with the BLYP functional using various basis sets leads to the cyclic structure of the dimer (cf. Table II), which contradicts the *ab initio* results. All the respective vibrational frequencies are positive, indicating that this structure corresponds to the energy minimum. The only exception represents the 6-31 + + G** basis set that gives bent structure more stable than the cyclic one. With Becke3LYP and Becke3P86 functionals, the cyclic structure (minimum) is found only for the 6-31G* and 6-31G** basis sets. Applying larger basis sets yields a bent structure of the dimer; vibrational analysis confirmed that this structure corresponds to an energy minimum. The geometry and energy characteristics of $(HF)_2$ are shown in Table II. Passing to larger basis sets results in an intermolecular distance increase and intramolecular distance decrease. Stabilization energy is, as with water dimer, reduced when enlarging the basis set. Our results agree will with that of ref. 20b, in which $(HF)_2$ was studied using nine various functionals. Working with the 6-31 + + G** basis set and BLYP functional, the bent structure of the dimer was found[20b] to be a global minimum.

TABLE I.
Geometry[a] (A, deg) and Energy (kcal / mol) Characteristics of the C_s Linear Structure of the Water Dimer[a] for Different DFT Functionals and Basis Sets.

Functional	Basis Set	R	r_1	r_2	r_3	α_1	α_2	α_3	α_4	$-\Delta E$	$-\Delta E_{cp}$[b]
BLYP	6-31G*[c]	2.867	0.988 (0.980)	0.979	0.982	17	103 (103)	81	103	7.8	—
	6-31G**[c]	2.890	0.985 (0.976)	0.975	0.978	14	103 (103)	85	103	7.7	—
	6-31 + + G**	2.912	0.985 (0.975)	0.976	0.976	5	105 (105)	120	105	5.6	4.8
	D95**	2.880	0.987 (0.977)	0.976	0.978	7	105 (104)	110	104	6.5	—
	D95(2*d*,2*p*)	2.912	0.983 (0.974)	0.973	0.975	4	104 (104)	110	104	6.2	—
Becke3LYP	6-31G*[c]	2.861	0.977 (0.969)	0.968	0.970	12	104 (104)	93	104	7.7	—
	6-31G**[c]	2.875	0.973 (0.965)	0.964	0.967	12	104 (104)	93	104	7.6	—
	6-31 + + G**	2.886	0.973 (0.964)	0.964	0.966	5	106 (106)	120	106	6.0	5.2
	D95**	2.868	0.975 (0.966)	0.965	0.967	5	105 (105)	116	105	6.6	—
	D95(2*d*,2*p*)	2.889	0.972 (0.963)	0.962	0.965	4	105 (105)	113	105	6.1	—
Becke3P86	6-31G*	2.835	0.976 (0.966)	0.965	0.968	10	104 (104)	98	104	7.6	5.8
	6-31G**	2.845	0.972 (0.962)	0.961	0.964	10	104 (104)	98	104	7.5	—
	6-31 + + G**	2.845	0.973 (0.962)	0.962	0.964	4	106 (106)	120	106	6.2	5.4
	D95**	2.834	0.974 (0.963)	0.962	0.965	5	105 (105)	116	105	6.6	—
	D95(2*d*,2*p*)	2.856	0.971 (0.961)	0.960	0.962	5	104 (105)	110	105	6.0	5.0

The numbers of parentheses correspond to the characteristics of isolated water.
[a]Cf. Figure 1a.
[b]Function counterpoise procedure employed.
[c]One imaginary frequency.

The potential energy surface of $(HF)_2$ is well known from MO calculations,[18] and it is the bent structure that corresponds to the global minimum. A cyclic structure is energetically less stable, and one imaginary frequency indicates that it corresponds to the saddle point. The MP4 stabilization energy of the bent dimer determined with the extended basis set[18] amounts to 3.7 kcal/mol. The MP2 geometry evaluated with the extended basis set is as follows[18]: R (2.76 Å), Δr (0.006 Å), α (112°), β (6°). The DFT intermolecular distance is underestimated, while the prolongation of the HF bond is overestimated; the situation is thus similar as for the water dimer. The DFT stabilization energy calculated with D95(2*s*,2*p*) is larger than the reference value mentioned earlier.

In contrast of $(HF)_2$, the gradient optimization of $(HCl)_2$ with various functionals and basis sets leads to the bent structure of the dimer. Positive vibrational frequencies of the dimer indicate that the stationary points correspond to the energy minimum. The geometry and energy characteristics of the bent $(HCl)_2$ dimer are given in Table II; these characteristics vary with various functionals

TABLE II.
Geometry[a] (A, deg) and Energy (kcal / mol) Characteristics of the $(HF)_2$ and $(HCl)_2$ Dimers for Different DFT Functionals and Basis Sets.

Dimer[a]	Funtional	Basis Set	R	r_1	r_2	r^b	α	β	$-\Delta E$	$-\Delta E_{cp}{}^c$
$(HF)_2$	BLYP	6-31G*	2.475	0.956	0.946	0.946	44.7	44.5	11.0	—
		6-31G**	2.485	0.946	0.946	0.936	44.6	44.5	10.7	—
		6-31 + + G**	2.757	0.942	0.947	0.939	111.6	7.5	4.9	4.4
		D95**	2.567	0.947	0.947	0.939	47.1	46.9	6.8	—
		D95(2*d*,2*p*)	2.596	0.942	0.942	0.935	47.1	47.1	6.4	—
	Becke3LYP	6-31G*	2.476	0.943	0.943	0.935	46.1	46.0	9.9	—
		6-31G**	2.488	0.933	0.933	0.925	46.3	46.2	9.6	—
		6-31 + + G**	2.730	0.931	0.935	0.928	113.4	7.5	5.2	4.8
		D95**	2.659	0.932	0.936	0.928	107.5	8.3	7.0	—
		D95(2*d*,2*p*)	2.676	0.927	0.932	0.925	106.3	7.5	6.7	—
	Becke3P86	6-31G*	2.458	0.941	0.941	0.931	46.1	45.9	8.9	—
		6-31G**	2.473	0.930	0.930	0.922	46.1	46.0	8.7	—
		6-31 + + G**	2.696	0.928	0.933	0.925	111.7	7.7	5.1	4.7
		D95**	2.642	0.929	0.934	0.925	107.7	7.9	6.5	—
		D95(2*d*,2*p*)	2.654	0.925	0.930	0.921	106.1	7.1	6.2	4.8
$(HCl)_2$	BLYP	6-31G*	3.878	1.303	1.307	1.302	94.4	6.3	1.8	—
		6-31G**	3.841	1.299	1.304	1.297	94.3	6.2	1.8	—
		6-31 + + G*	3.894	1.300	1.304	1.299	96.5	5.9	1.3	1.1
		D95**	3.824	1.300	1.306	1.298	89.6	7.1	2.2	—
		D95(2*d*,2*p*)	3.815	1.293	1.299	1.291	90.6	3.7	2.2	—
	Becke3LYP	6-31G*	3.860	1.291	1.295	1.290	94.9	6.9	1.8	—
		6-31G**	3.828	1.288	1.292	1.287	94.7	6.6	1.9	—
		6-31 + + G**	3.864	1.289	1.293	1.288	98.6	5.4	1.8	1.4
		D95**	3.815	1.290	1.295	1.289	90.6	7.5	2.2	—
		D95(2*d*,2*p*)	3.801	1.284	1.289	1.282	86.8	7.8	2.2	—
	Becke3P86	6-31G*	3.779	1.287	1.292	1.286	94.8	6.6	1.9	—
		6-31G**	3.744	1.284	1.290	1.282	94.7	6.3	2.1	—
		6-31 + + G**	3.760	1.285	1.291	1.284	96.1	6.0	1.9	1.7
		D95**	3.738	1.287	1.293	1.285	90.4	7.4	2.3	—
		D95(2*d*,2*p*)	3.726	1.282	1.288	1.280	90.2	4.7	2.2	1.7

[a] Cf. Figure 1b.
[b] Isolated system.
[c] Function counterpoise procedure employed.

and basis sets less than for $(HF)_2$. Here, the stabilization energy increases with increasing basis set size. The cyclic structure of the $(HCl)_2$ dimer corresponds to the saddle point; one imaginary vibrational frequency was found at the BLYP/6-31G* level. The energy barrier between the minimum and the saddle point amounts to 0.64 kcal/mol (BLYP/6-31G*).

The bent structure of $(HCl)_2$ corresponds to the global minimum; this was confirmed theoretically and experimentally.[21] The following geometry [R (3.9 Å), α (89°), β (6°)] and stabilization energy (1.7 kcal/mol) was found[22] using the averaged coupled pair functional. The *ab initio* value of the energy barrier (difference between the minimum and the saddle point) lies[21] between 0.17 and 0.24 kcal/mol. Therefore, the DFT geometry and energy characteristics agree very well with values given earlier in this article; the same is true of the energy barrier.

Formamide ··· formamidine Complex

The H-bond pattern of formamide ··· formamidine (cf. Fig 1c) is the same as that of adenine ··· thymine. Investigation of the dynamics of adenine ··· thymine (as well as of other DNA base pairs) requires the performance of a series of gradient optimizations. Gradient optimization of a DNA base pair with basis set of DZ or even DZ + P quality is still rather tedious, and the idea

of performing these calculations with DFT methods is thus tempting.

Table III contains intermolecular and selected intramolecular geometry characteristics and the stabilization energy of the cyclic structure of formamide ··· formamidine evaluated with the DFT, HF, and MP2 methods using various basis sets. It can be seen from the table that both the geometry and energy characteristics of the cluster vary only slightly with DFT functionals and basis sets. The DFT geometry characteristics agree well with the HF as well as the MP2 data. The only difference concerns the change of N—H bonds on formation of H bonds. Whereas HF and MP2 lead to prolongation of the N—H bonds, DFT predicts almost no changes in these bonds. The DFT stabilization energy lies between the HF and MP2 stabilization energies.

DFT results for the present cluster are rather encouraging and support the application of DFT for larger cyclic clusters having more H bonds (e.g., DNA base pairs).

IONIC CLUSTER

$LiOH_2^+$, $FHOH^-$

The C_{2v} and C_s (linear) structures of $LiOH_2^+$ and $FHOH^-$ clusters (cf. Figs. 1d and 1e) were most stable and both correspond to an energy minimum. Geometries and stabilization energies evaluated with various functionals using the 6-31G* basis set are presented in Table IV for both clusters. It is clear from the table that neither the geometries nore the stabilization energies are sensitive to the functionals.

The DFT geometry and energy characteristics for $LiOH_2^+$ agree well with the MP2/6-31G* ones. For $FHOH^-$, the MP2 geometry data are well reproduced by the DFT method, while the DFT stabilization energies are slightly larger than the MP2 value.

Good agreement between DFT and *ab initio* geometry and energy characteristics was found also for $Au^+ \cdots OH_2$ (ref. 9).

ELECTROSTATIS CLUSTERS

Benzene Dimer

The study of the benzene dimer is important because the dimer represents a prototype for interactions between aromatic π-systems. The main part of stabilization of the dimer originates in the correlation effects, but the electrostatic quadrupole–quadrupole term also plays a role. Three various structures—sandwich (Fig. 1f), T-shaped (Fig. 1g), and parallel-displaced (Fig. 1h)—were investigated with various functionals and mainly with the 6-31G* basis set; the interaction energies are presented in Table V. Point-by-point optimization

TABLE III.

Geometry (Å, deg) and Energy Characteristics (kcal / mol) of the Cyclic Structure of the Formamide ··· Formamidine[a] for Different Functionals and Basis Sets; HF and MP2 Characteristics Are Also Presented.

Functional	Basis Set	$N_1—O_8$	$N_1—H_4$	$N_{10}—N_3$	$N_{10}—H_{12}$	$N_1—O_8—C_9$	$-\Delta E$
BLYP	6-31G*	2.913	1.018 (1.018)	2.926	1.018 (1.019)	119	18.1
Becke3LYP	6-31G*	2.904	1.010 (1.010)	2.922	1.009 (1.011)	118	18.0
Becke3P86	6-31G*	2.858	1.009 (1.009)	2.872	1.008 (1.010)	119	18.6
Becke3P86	D95**	2.812	1.009 (1.009)	2.830	1.008 (1.010)	118	17.4
HF	6-31G*	3.031	1.003 (0.994)	3.063	1.010 (0.993)	119	14.5
HF	D95**	3.028	1.003 (0.994)	3.055	1.010 (0.995)	121	12.5
HF	D95(2*d*,2*p*)	3.025	0.999 (0.991)	3.075	1.005 (0.992)	121	12.7
MP2	6-31G*	2.953	1.024 (1.010)	2.966	1.034 (1.011)	118	25.7

The numbers of parentheses correspond to the characteristics of isolated system.
[a]Cf. Figure 1c.

TABLE IV.

Geometry (Å, deg) and Energy Characteristics[a] (kcal / mol) of the $LiOH_2^+$ and $FHOH^-$ Clusters for Different Functional with the 6-31G* Basis Set. MP2 characteristics are also presented.

Cluster[a]	Functional	R	r_1	r_2	α	β	$-\Delta E$
$LiOH_2^+$	BLYP	1.843	0.982	—	106	—	43.3
			(0.980)		(103)		
	Becke3LYP	1.838	0.973	—	106	—	42.8
			(0.969)		(104)		
	Becke3P86	1.844	0.971	—	106	—	40.7
			(0.966)		(104)		
	MP2	1.865	0.976	—	106	—	41.6
			(0.969)		(104)		
$FHOH^-$	BLYP	2.440	1.155	0.983	4	92	53.9
	Becke3LYP	2.407	1.128	0.971	4	94	50.7
	Becke3P86	2.390	1.134	0.967	4	98	50.4
	MP2	2.414	1.106	0.969	4	94	45.0
			(0.969)				

Numbers in parentheses correspond to isolated water.
[a]Cf. Figures 1d and 1e.

TABLE V.

Interaction Energy (kcal / mol) of the Various Structures of the Benzene Dimer Evaluated for Different DFT Functionals with the 6-31G* Basis Set.

Structure[a]	Functional	R(A)	R_1(A)	ΔE	ΔE_{cp}[b]
Sandwich	BLYP	3.6		5.03	
		4.0		1.66	
		4.4		0.90	
		5.0		0.66	
		6.0		0.28	
	Becke3P86	4.0		1.46	
		5.0		0.85	
		6.0		0.37	
T-shape	Becke3P86	4.5		2.61	4.06
		5.0		−0.17	0.46
		5.3		−0.78	0.00
		5.5		−0.79	−0.26
				−0.43[c]	−0.17[c]
		5.6		−0.61	−0.29
		5.7		−0.41	−0.25
		6.0		−0.18	−0.06
Parralel displaced	Becke3P86	2.8	4.7	−0.25	
		3.0	4.7	−0.45	
		3.0	4.5	−0.37	0.42
		3.0	4.8	−0.50	0.14
				−0.34[c]	
				−0.40[d]	
		3.0	4.9	−0.48	0.11
		3.2	4.7	−0.32	

[a]Cf. Figures 1f, 1g, and 1h.
[b]Function counterpoise procedure employed.
[c]D95** Basis set used.
[d]D95(2*d*,2*p*) basis set used.

revealed a purely repulsive potential energy curve for the sandwich structure. Very similar results were obtained with the BLYP and Becke3P86 functionals. For the T-shaped structure, only the latter functional was employed and minima of 0.79 and 0.43 kcal/mol at 5.5 Å resulted if the 6-31G* and D95** basis sets were used, respectively. Exclusion of BSSE reduces the minimum well to 0.26 and 0.17 kcal/mol, respectively. For parallel-displaced structures, the point-by-point optimization (Becke3P86/6-31G*) leads to an energy minimum of 0.5 kcal/mol. Exclusion of BSSE shifted, however, the interaction energies to positive values. For the parallel-displaced structure, the effect of larger basis sets was also studied. For the minimal geometry found with the 6-31G* basis set, the Becke3P86 calculations with D95** and D95(2*d*,2*p*) basis sets were performed. The resulting stabilization energies differ only slightly from that found at the Becke3P86/6-31G* level. The potential energy surface of the benzene dimer was studied at the MP2/DZ(2*d*,2*p*) level and the following minima were found[23]: sandwich structure (3.9 Å, −0.85 kcal/mol), T-shaped structure (5.0 Å, −2.11 kcal/mol), parallel-displaced structure (3.5 Å, 1.6 Å, −2.28 kcal/mol). Evidently, the DFT interaction energies are too small, which may be due to neglect of the dispersion energy in the presently used DFT functionals. The shallow minima found for the T-shaped structure could be caused by the electrostatic quadrupole–quadrupole interaction. This interaction is covered by the *ab initio* self-consistent field (SCF) calculation and, seemingly, it is also covered by the DFT calculation. As a consequence of quadrupole–quadrupole electrostatic repulsion and nonconsidered dispersion energy, a repulsive DFT interaction energy results for the sandwich structure of the benzene dimer. Finally, the quadrupole–quadrupole electrostatic attraction is responsible for the existence of the shallow minimum found for the parallel-displaced structure. Comparing the MP2 and DFT results for this structure, we found that the planar displacement (R_1 in Fig. 1h) predicted by DFT is considerably larger than that found by MP2. It was shown[23] that the dispersion energy reduces the displacement. The multipole analysis performed for this structure gives larger values of displacement (in comparison with MP2), which are comparable to the DFT values. It could thus be concluded that the presently considered DFT functionals do not cover the dispersion energy, while the electrostatic interaction is described properly.

Ethylene Dimer

In light of results obtained for the benzene dimer, we did not scan the ethylene dimer potential energy surface. Rather, we performed a detailed investigation of the dependence of the interaction energy of the dimer on the basis set and the functional. A sandwich structure (cf. Fig. 1i) with intermolecular separation of 3.5 Å was considered. Figure 2a compares the basis set dependence of the SCF interaction energy, counterpoise-corrected SCF interaction energy, Becke3P86 interaction energy, and counterpoise-corrected Becke3P86 interaction

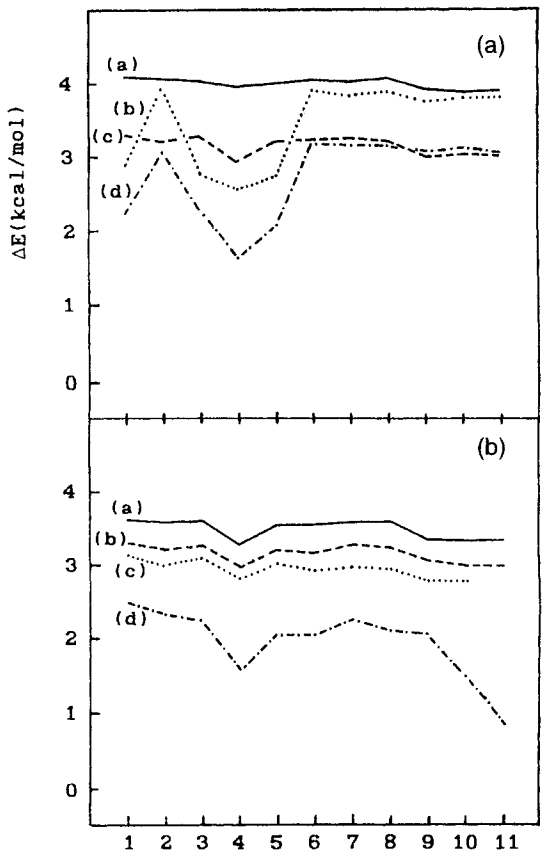

FIGURE 2. (a) Basis set dependence of counterpoise corrected SCF interaction energy (a), SCF interaction energy (b), counterpoise corrected Becke3P86 interaction energy (c), and Becke3P86 interaction energy (d) for sandwich structure of the ethylene dimer evaluated for 11 various basis sets: 1 (6-31G*), 2 (6-31 + G), 3 (6-31G*), 4 (6-31G* (0.25)), 5 (6-31G**), 6 (6-31 + G*), 7 (DZP), 8 (DZ2P), 9 (DZ + P), 10 (6-211 + + G**), 11 (6-31 + +(3*df*,2*p*)). (b) Basis set dependenace of counterpoise corrected BLYP (a), Becke3LYP (b), Becke3P86 (c), and MP2 (d) interaction energies for sandwich structure of the ethylene dimer evaluated for 11 barious basis sets mentioned in Fig. 2a.

energy, evaluated with 11 various basis sets. It is evident that the courses of counterpoise corrected and counterpoise uncorrected interaction energies are very similar. This gives clear evidence that the DFT interaction energy and SCF interaction energy exhibit similar basis-set extension dependence. The use of the function counterpoise method is therefore essential for evaluation of the DFT interaction energy. It must be mentioned, however, that all the basis sets used were optimized for the Hartree-Fock method. It is thus possible to expect that optimizing basis sets for DFT will result in smaller BSSE; this especially concerns smaller basis sets. Figure 2b demonstrates the basis-set dependence of corrected BLYP, Becke3LYP, Becke3P86, and MP2 interaction energies. It becomes evident that all three DFT interaction energies are very similar. The MP2 interaction energy is different, especially for larger basis sets containing diffuse the polarization functions. The difference between the DFT and MP2 interaction energies again provides evidence for neglecting the dispersion energy in the DFT interaction energy.

LONDON CLUSTERS

Ne_2, Ar_2

For Ne and Ar 6-311G(2*df*), [5*s*4*p*2*d*1*f*] and 6-311G(2*df*), [7*s*4*p*2*d*1*f*] basis sets were used, respectively. In the case of Ar ··· Ar, a purely repulsive interaction energy was obtained (see Table VI); exclusion of BSSE makes the interaction energy more repulsive. Both the basis sets used as well as all the three functionals give very similar interaction energies. The fact that no minimum was found on the potential energy curve was expected because the Ar ··· Ar attraction originates exclusively in the dispersion energy. For Ne ··· Ne, a shallow minimum was obtained at about 3.0 Å, and it remains even after excluding the BSSE (cf. Table VI). This conclusion is not affected by basis sets or functionals. We do not have an explanation for the existence of this minimum since, as was shown earlier, the dispersion energy is not covered by the currently available DFT functionals. Our results agree fully with those of the ref. 24, in which He_2, Ne_2, and Ar_2 were investigated by the DFT method using Becke exchange, BLYP, and Dirac-Slater (DS) functionals. The first two functionals yield (after counterpoise correction) a purely repulsive potential. On the other hand, the simplest DS functional gives strongly overestimated potential energy minima. This overestimation originates,[24] however, from an overlap effect and not from dispersion attraction.

Benzene ··· *X*(*X* = Ne, Ar)

In light of the results obtained for $(benzene)_2$, $(Ar)_2$ and $(Ne)_2$, we expected no minimum on the C_{6v} potential energy curve of benzene ··· Ne and benzene ··· Ar (cf. Fig. 1j). It can be seen from Table VII that a purely repulsive potential energy curve is found for the latter cluster even for an extended basis set having two sets of polarization *d* functions on C and Ar and *p* functions on H. The interaction energies are again very similar for all the three functionals employed. The most accurate calculations for the cluster,[23] taking the correlation

TABLE VI.
Interaction Energy (kcal / mol) of the Ar ··· Ar and Ne ··· Ne Clusters Evaluated for Different DFT Functionals and Basis Sets.

	Ar ··· Ar				Ne ··· Ne			
Functional	BLYP		Becke3LYP	Becke3P86	BLYP		Becke3LYP	Becke3P86
Basis Set	7*s*4*p*2*d*1*f*	6-311G(2*df*)	7*s*4*p*2*d*1*f*	7*s*4*p*2*d*1*f*	5*s*4*p*2*d*1*f*	6-311G(2*df*)	5*s*4*p*2*d*1*f*	5*s*4*p*2*d*1*f*
R(Å)								
2.0	—	—	—	—	8.5 (9.8)	7.6 (9.4)	8.0	8.7 (9.2)
2.3	—	—	—	—	1.2 (2.1)	—	1.1 (1.8)	1.9 (2.3)
2.5	20.4 (21.4)	20.8 (21.1)	—	—	−0.1 (1.0)	−0.4 (0.8)	0.0	0.6 (1.2)
3.0	4.0 (4.4)	4.0 (4.2)	3.3	3.1	−0.9 (0.1)	−0.4 (−0.1)	−0.6	−0.3 (0.2)
3.5	1.2 (1.3)	1.2 (1.2)	0.9	0.9	−0.6 (−0.1)	−0.2 (−0.2)	−0.4	−0.3 (−0.1)
4.0	0.8 (1.0)	0.7 (1.0)	0.5	0.6	−0.4 (−0.1)	−0.2 (−0.2)	−0.3	−0.2 (0.0)
5.0	0.2 (0.7)	0.1 (0.7)	0.1	0.1	—	—	—	—

Numbers in parentheses correspond to the BSSE corrected interaction energy.

TABLE VII.
Interaction Energy (kcal / mol) of the C_{6v} Structure of Benzene ··· Ar Cluster[a] Evaluated for Different Functionals and Basis Sets.

Functionals	BLYP		Becke3LYP	Becke3P86
Basis Set	6-311G*	6-311G (2*d*,2*p*)	6-311G*	6-311G*
R(Å)				
2.8	8.3 (8.8)	8.1 (8.7)	7.1 (7.6)	5.9 (6.3)
3.5	1.4 (1.6)	1.3 (1.5)	0.8 (1.0)	0.7 (0.8)
4.5	0.3 (0.4)	0.3 (0.3)	0.2 (0.2)	0.3 (0.3)

Numbers of parentheses correspond to the BSSE corrected interaction energy.
[a]Cf. Figure 1j.

energy into account, give an energy minimum of about 1 kcal/mol at a distance of 3.5 Å.

Benzene ··· Ne is slightly different because (see Table VIII) shallow minima were localized on the C_{6v} potential energy curves. Only the Becke3P86 functional gives a purely repulsive interaction energy. Exclusion of BSSE removes, however, these shallow minima. *Ab initio* calculations covering the correlation energy predict[23] a minimum of about 0.3 kcal/mol for 3.4 Å.

Conclusions

1. Reliable geometry and energy characteristics were obtained for an H-bonded water dimer and HF dimer with Becke3LYP and Becke3P86 functionals if larger basis sets [6-31 + + G**, D95**, D95(2*d*,2*p*)] were used. The cyclic structure of the $(HF)_2$ dimer is incorrectly predicted by the BLYP functional to be the global minimum; a bent structure as the global minimum results only if the 6-31 + + G** basis set is applied. Reliable characteristics of the $(HCl)_2$ dimer were obtained with all three functionals and all basis sets. DFT intermolecular distances are slightly underestimated, while the prolongation of the subsystem bond upon formation of the H bond is too large.
2. Encouraging results were obtained for the cyclic formamide ··· formamidine cluster with all three functionals, even with the smallest basis set (6-31G*).
3. Reliable characteristics of ionic clusters were obtained with all three functionals.
4. The dispersion energy is not covered in DFT methods using BLYP, Becke3LYP, and Becke3P86 functionals. Similar conclusion resulted from the literature[24] when using the Becke exchange functional. Other energy contributions, such as electrostatic, are properly considered. The DFT interaction energy usually lies between the HF and MP2 values. It would be desirable to develop a new functional which cover dispersion energy in DFT calculations.
5. The DFT interaction energy exhibits the same basis set extension dependence as the HF interaction energy. The DFT basis set superposition error should be eliminated by using the Boys-Bernardi function counterpoise method.
6. To summerize the applicability of DFT for molecular cluster, the method could give reliable results for H-bonded and ionic clusters, and its use especially for cyclic clusters with multiple H bonds seems promising. DFT with currently available functionals does not cover the dispersion energy and thus fails for London clusters and for those electrostatic clusters in which the dispersion energy is

TABLE VIII.
Interaction Energy (kcal / mol) of the C_{6v} Structure of Benzene ··· Ne Cluster[a] Evaluated for Different Functionals and Basis Sets.

Functional	BLYP	Becke3LYP	Becke3P86
Basis Set	6-31G*	6-31G*	6-31G*
R(Å)			
2.5	0.8 (5.0)	0.8 (4.3)	1.8 (4.8)
2.8	−0.6 (2.1)	−0.6 (1.7)	0.3 (2.2)
3.5	−0.2 (0.1)	−0.2 (0.1)	0.1 (0.4)
4.5	0.0 (0.0)	0.0 (0.0)	0.0 (0.0)

Numbers in parentheses correspond to the BSSE corrected interaction energy.
[a]Cf. Figure 1j.

dominant. The method also fails for charge-transfer complexes, for which it predicts unrealistically deep energy minima.[25]

References

1. R. O. Jones and O. Gunnarsson, *Rev. Mod. Phys.*, **61**, 689 (1989).
2. J. Andzelm and E. Wimmer, *J. Chem. Phys.*, **96**, 1280 (1992).
3. B. G. Johnson, P. M. W. Gill, and J. A. Pople, *J. Chem. Phys.*, **98**, 5612 (1993).
4. F. Sim, A. St-Amant, I. Papoi, and D. R. Salahub, *J. Am. Chem. Soc.*, **114**, 4391 (1992).
5. K. Laasonen, M. Parrinello, R. Car, Ch. Lee, and D. Vanderbilt, *Chem. Phys. Lett.*, **207**, 208 (1993).
6. T. Zhu and W. Yang, *Int. J. Quantum Chem.*, **49**, 613 (1994).
7. C. Mijoule, Z. Latajka, and D. Borgis, *Chem. Phys. Lett.*, **208**, 364 (1993).
8. (a) J. Florian and B. Johnson, *J. Phys. Chem.*, **99**, 5899 (1995); (b) M. Kieninger and S. Suhai, *Int. J. Quantum Chem.*, **52**, 465 (1994); (c) K. Kim and K. D. Jordan, *J. Phys. Chem.*, **98**, 10089 (1994); (d) B. Santamaria and A. Vázquer, *J. Comp. Chem.*, **15**, 981 (1994).
9. J. Hrušák, D. Schröder, and H. Schwarz, *Chem. Phys. Lett.*, **225**, 416 (1994).
10. S. F. Boys and F. Bernardi, *Mol. Phys.*, **19**, 553 (1970).
11. J. Sauer, P. Ugliengo, E. Garrone, and V. R. Saunders, *Chem. Rev.*, **94**, 2095 (1994).
12. M. J. Frisch, G. W. Trucks, M. Head-Gordon, P. M. W. Gill, M. W. Wong, J. B. Foresman, B. G. Johnson, H. B. Schlegel, M. A. Robb, E. S. Replogle, R. Gomperts, J. L. Andres, K. Raghavachari, J. S. Binkley, C. Gonzalez, R. L. Martin, D. J. Fox, D. J. Defrees, J. Baker, J. J. P. Stewart, and J. A. Pople, Gaussian 92/DFT, Revision A, Gaussian, Inc., Pittsburgh, PA, 1992.
13. A. D. Becke, *Phys. Rev.*, **A38**, 3098 (1988).
14. C. Lee, W. Yang, and R. G. Parr, *Phys. Rev.*, **B37**, 785 (1987).
15. B. Miehlich, A. Savin, H. Stoll, and H. Preuss, *Chem. Phys. Lett.*, **157**, 200 (1989).
16. A. D. Becke, *J. Chem. Phys.*, **98**, 5648 (1994).
17. P. J. Stevens, F. J. Devlin, C. F. Chablowski, M. J. Frisch, *J. Chem. Phys.*, submitted for publication.
18. M. J. Frisch, J. E. Del Bene, J. S. Binkley, and H. F. Schaefer III, *J. Chem. Phys.*, **84**, 2279 (1986).
19. D. Feller, *J. Chem. Phys.*, **96**, 6104 (1992).
20. (a) Y.-B. Wang, F.-M. Tao, and Y.-K. Pan, *J. Mol. Struct. (THEOCHEM)*, **309**, 235 (1994); (b) Z. Latajka and Y. Bouteiller, *J. Chem. Phys.*, **101**, 9793 (1994).
21. A. B. McCoy, Y. Hurwitz, and R. B. Gerber, *J. Phys. Chem.*, **97**, 12516 (1993).
22. A. Karpfen, P. R. Bunker, and P. Jensen, *Chem. Phys.*, **149**, 299 (1991).
23. P. Hobza, H. L. Selzle, and E. W. Schlag, *Chem. Rev.*, **94**, 1767 (1994).
24. S. Kristyán and P. Pulay, *Chem. Phys. Lett.*, **229**, 175 (1994).
25. (a) D. Salahub, Lecture at the 8th International Congress on Quantum Chemistry, Prague, 1994; (b) E. Ruiz, D. R. Salahub, and A. Vela, *J. Am. Chem. Soc.*, **117**, 1141 (1995).